On-off QD switch that memorizes past recovery from quenching by diazonium salts†

Marta Liras,* María González-Béjar and J. C. Scaiano*

Received 23rd February 2010, Accepted 14th May 2010
DOI: 10.1039/c003490h

The understanding of the interaction of CdSe/ZnS semiconductor quantum dots (QD) with their chemical environment is fundamental, yet far from being fully understood. *p*-Methylphenyldiazonium tetrafluoroborate has been used to get some insight into the effect of diazonium salts on the spectroscopy of QD. Our study reveals that the surface of CdSe/ZnS quantum dots can be modified by diazonium salts (although not functionalized), showing and on-off fluorescence behaviour that memorizes past quenching recoveries. Facile modification of the surface confers protection against quenching by new molecules of diazonium salt and other known quenchers such as 4-amino-TEMPO. The reaction mechanism has been explored in detail by using different spectroscopic techniques. At the first time after addition of diazonium salt over QD the fluorescent is turned off with Stern–Volmer behaviour; the fluorescence recovers following irradiation. Subsequent additions of diazonium salts do not cause the same degree of quenching. We have noted that the third addition (following two cycles of addition and irradiation) is unable to quench the fluorescence. Monitoring the process using NMR techniques reveals the formation of *p*-difluoroborane toluene as a result of the irradiation of diazonium-treated QD; the treatment leads to the fluorination of the QD surface.

Introduction

Semiconductor nanocrystals or quantum dots (QD) have attracted much attention due to their size-dependent physical properties originating from quantum confinement.[1,2] A wide range of applications such as QD laser,[3] biological markers,[4] light emiting diodes (LEDs)[5,6] have been investigated. These semiconductor nanoparticles exhibit a broad excitation spectra coupled with a narrow size-tunable luminescence emission, high brightness and good photostability.[1] QD are formed by atoms from group II (alkyl metals, metal oxides or organic salts) and group VI (Se, S and Te). The addition of an inorganic shell (*e.g.*, ZnS) leads to core–shell QD, which have high fluorescence quantum yield and stability.[7,8]

QD are usually synthesized using trioctylphosphine oxide (TOPO) and trioctylphosphine (TOP) as ligands, which make them soluble in organic solvents. Understanding ligand exchange dynamics and mechanisms in which the TOPO ligands on the QD surface can be replaced with the ligand of choice has become crucial since one could obtain, for example, quantum dots soluble in water or make them amenable to chemical reactions as desired. Thiols have proven useful in ligand exchange due to their high affinity for the particle surface.[9] Alternatives to thiols include carbodithioates,[10] peptides,[11] and oligomeric phosphines.[12] The optical properties of QDs are quite sensitive to their capping ligand, highlighting the importance of surface phenomena. The presence of different molecules close to the QD can change their luminescent properties and these changes can be used for different applications. Fluorescence quenching or enhancement can be observed as a result of small molecule-QD interactions.

Diazonium salts readily lose N_2 by either direct photoexcitation or through electron transfer processes.[13] Direct photoexcitation yields highly reactive aryl carbocations, while the (frequently favored) electron transfer process tends to yield aryl radicals also highly reactive towards a wide range of substrates, both organic and inorganic (Scheme 1).

Possible electron donors include metal and semiconductor surfaces, where electrochemistry has proven a valuable tool for surface derivatization.[14] In this case electron transfer from the cathode leads to rapid nitrogen loss following one electron reduction; aryl radicals are thus generated at the electrode surface, where they can react in competition with diffusion into the bulk liquid phase. There are also examples of spontaneous reactions in different materials such as nanotubes,[15–17] metals such as Au, Pb and Pt,[18] and semiconductors such as silicon and GaAs.[19] We wondered what effect diazonium salts could have on the spectroscopy of semiconductor nanocrystals, and whether photoinduced electron transfer could be used to

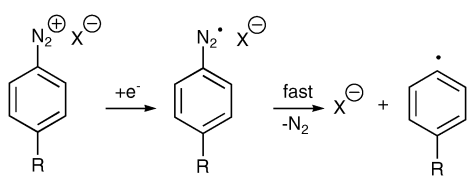

Scheme 1 Electron transfer processes of diazonium salts.

Department of Chemistry and Centre for Catalysis Research and Innovation, University of Ottawa, Ottawa, Ontario, K1N 5N6. E-mail: tito@photo.chem.uottawa.ca; Fax: +1 613 562 5633

† Electronic supplementary information (ESI) available: Pictures of QD solutions after additions of compound **1**, lifetime distribution for QD_{610} and QD_{546}, fluorescence recovery comparison for QD_{610} under UVB and UVA illumination, evolution of QD_{546} fluorescence and data for core QD_{558}. See DOI: 10.1039/c003490h

modify these particles. With these ideas in mind, we explored the interaction of core–shell CdSe/ZnS quantum dots (QD) with a simple diazonium salt (R = CH_3 in Scheme 1).

Experimental

General details

p-Toluidine and 4-amino-TEMPO (4aT) were purchased from Aldrich and used without further purification. CdSe/ZnS QD were purchased from Evident Technologies and the experiments were carried out in toluene solution at room temperature. In order to remove excess TOPO free in solution, the QD_{610} and QD_{546} (where the subscript identifies the maximum emission wavelength) were precipitated with methanol, centrifuged and redissolved in the same amount of toluene. The concentration of the new solution was determinated using a literature protocol.[20]

Core CdSe QD_{558} were synthesized as previously reported.[21] Absorption spectra were recorded using a Cary-50 UV-Visible spectrometer. Fluorescence was recorded with a Photon Technology International (PTI) spectrofluorometer. Fluorescence lifetime measurements were recorded using an Easylife LS (PTI) using a 490 nm pulsed LED and the appropriate filters for each case. In all cases the experimental error was $\leq 5\%$ (unless otherwise indicated). The irradiation of the samples was performed with Luzchem LZC-ORG photoreactor using 6 visible or UVA lamps. Dynamic light scattering measurements were recorded using Zetasizer Nano (ZS) apparatus from Malvern with the 4 mW, 633 nm He–Ne laser.

NMR spectra were obtained on a Bruker Avance-400 spectrometer at 400 MHz using $CDCl_3$ or methanol-d_4 as solvent without an internal standard.

Synthesis of *p*-tolyldiazonium tetrafluoroborate salt (1)[22]

To 1.98 g of boron trifluoride etherate (1.7 mL, 13.9 mmol) contained in a three-neck round-bottom flask fitted with two addition funnels and a reflux condenser connected to a gas buret was added 1 g (9.3 mmol) of *p*-toluidine in 10 mL of anhydrous THF. Prior to amine addition, the boron trifluoride etherate was cooled at −15 °C in an ice-acetone bath. If a solid amine-BF_3 complex formed, additional solvent or ethyl ether were added to produce a homogeneous solution. tert-Butyl nitrite 1.3 mL (11.6 mmol) in 5 mL of the same solvent was added dropwise to the rapidly stirred solution over a 10 min period. Following complete addition, the temperature of the reaction solution was maintained at −15 °C for 10 min and then allowed to warm to 5 °C in an ice-water bath over a 20 min period. A crystalline precipitate usually formed during the addition of tert-butyl nitrite, and following the 20 min period at 5 °C, precipitation was completed. The solid was filtered, washed with cold diethyl ether, air-dried, and weighed to afford 1.6 g (92% yield) of white needles. ^{1}H NMR (MeOD, 400 MHz): δ 8.47 (J = 8.4 Hz, d, 2H, *Ar*H), 7.78 (J = 8.4 Hz, d, 2H, *Ar*H), 2.63 (s, 3H, CH_3).

UV-Visible or steady state fluorescence quenching experiments

In a typical experiment, 2 mL of a toluene solution of QD 0.5 μM (for both UV-Visible and fluorescence spectroscopy) was prepared in a precision quartz cuvette. Added to the cuvette were varying amounts of a 2.02 mM or 20.2 mM fresh solutions of **1** in acetonitrile, such that the total volume added to each cuvette in each addition never exceeded 50 μL. In all UV-Visible and fluorescence experiments, **1** was added in the dark (and kept in the dark). Samples were exposed to illumination exclusively for the fluorescence recovery studies. For the experiments with 4-amino-TEMPO, aliquots of 2 μL of stock solutions (20 mM for high concentrations and 2 mM for lower ones) were added.

Characterization of *p*-difluoroborane toluene (2)

To a solution of 2.25 mL QD_{610} (23 μM) in $CDCl_3$, 21 μL of **1** (480 mM) were added in a NMR tube (final solution of **1** was 4.6 mM). The sample was irradiated for 3 h. The proccess (addition and irradiation) was repeated twice. Then, the sample was precipitated with deuterated methanol and centrifuged. The methanolic part was analyzed by NMR (Fig. 1). ^{1}H NMR (MeOD, 400 MHz): δ 7.18 (J = 8.4 Hz, d, 2H, *Ar*H), 7.10 (J = 8.4 Hz, d, 2H, *Ar*H), 2.21 (s, 3H, CH_3). ^{11}B NMR (MeOD, 128.4 MHz): δ 20.3 ppm. ^{19}F NMR (MeOD, 376.5 MHz): −152.46 ppm.

Result and discussion

The choice of core–shell CdSe/ZnS QD and the diazonium salt **1** for this study deserves some comment: core–shell QD of this type have proven quite stable,[1] highly luminescent, leading to numerous applications.[3–6] The synthesis of the diazonium salts is generally straightforward if the corresponding aromatic amine is available.[22] Thus, the *para*-CH_3 group in the diazonium salt selected is a representative substituent that can be easy detectable by ^{1}H-NMR. In our case *p*-$CH_3C_6H_5N_2^+$, BF_4^- (**1**) was synthesized from 4-aminotoluene as described in the

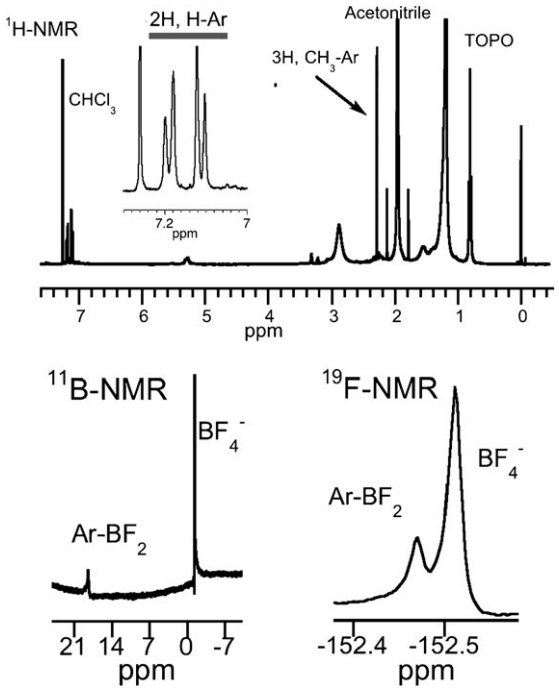

Fig. 1 Characterization of *p*-difluoroborane toluene **2** by NMR.

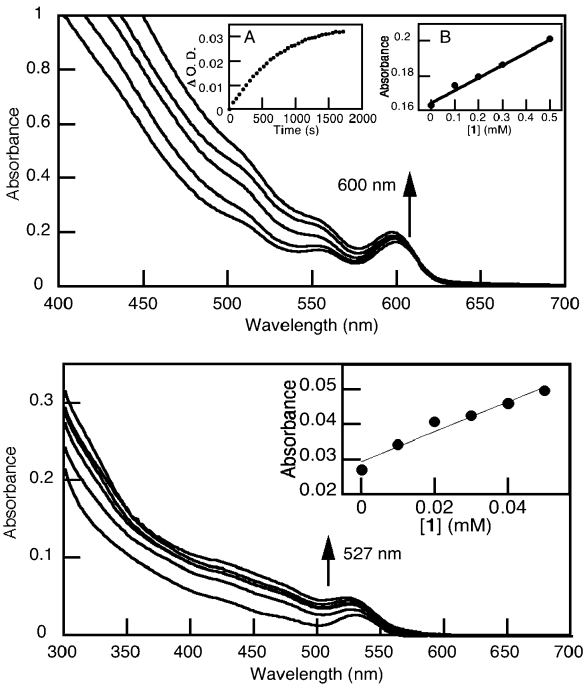

Fig. 2 Changes in absorption spectra for QD_{610} (top) and QD_{546} (bottom), both 0.5 μM in toluene upon addition of incremental amounts of **1**, and recorded 30 min after addition. Inset (top): A) QD_{610} absorption in the first exciton peak at different concentrations of **1** monitored until 1 h after addition. Inset: Absorbance changes in the first exciton peak for QD_{610} (top B) and QD_{546} (bottom) with incremental amounts of **1**.

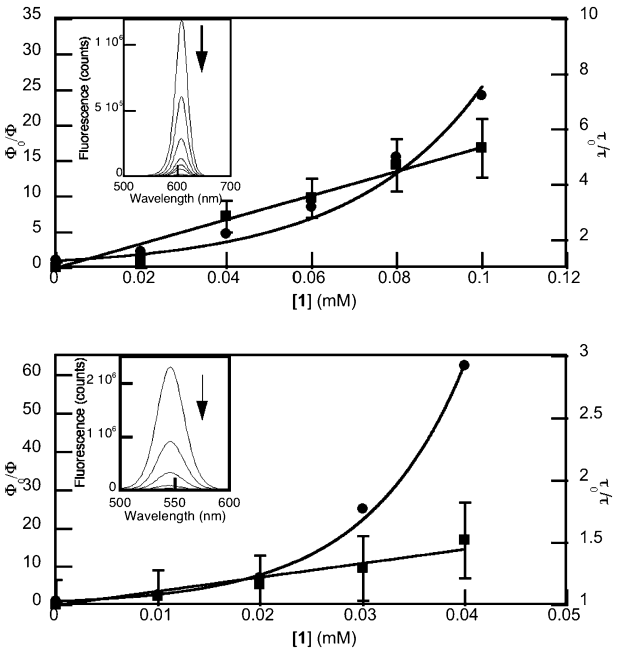

Fig. 3 Stern–Volmer plot of a QD_{610} solution (0.5 μM) in toluene (top) and QD_{546} solution (0.5 μM) in toluene (bottom). Insets: QD_{610} (top) and QD_{546} (bottom) emission spectra (top) upon incremental additions of **1**. The ratio is represented Φ_0/Φ by circles and τ_0/τ by squares.

experimental section. Commercial QD_{610} and QD_{546}, with TOPO (trioctylphosphine oxide) as stabilizer, were used in toluene. Addition of **1** to solutions containing QD (0.5 μM) results in a linear increase in absorbance for both, QD_{610} and QD_{546}, that is proportional to the concentration of **1** and is complete in less than an hour. The process follows first order kinetics with k (QD_{610}) = (1.3 ± 0.1) × 10^{-3} s^{-1}, as is illustrated in inset A and inset B in Fig. 2A, respectively.

Absorption spectra changes for QD upon addition of ligands has been mainly attributed to the QD high sensitivity to local changes in the environmental charge distribution.[21,23,24] Thus, Bawendi *et al*. have shown how *J*-aggregated cyanine dyes donors are electrostatically associated to the QD in solution *via* surface ligands producing a narrow-band absorption enhancement of colloidal quantum dots (QD) through efficient Förster resonance energy transfer (FRET).[24] We have recently shown that QD UV-Visible spectra undergo significant changes upon 7-mercapto-4-methylcumarin addition due to charge transfer interactions.[21] A possible origin for spectral changes would be Rayleigh scattering as a consequence of QD aggregation. However, all the solutions remained clear and stable (See Supporting Information Fig. S1–S3) at the concentrations used for this study. Further, it has been recently shown for PbSe that the rising absorption of the Q-PbSe suspension at short wavelengths is not due to Rayleigh scattering, but it reflects a strong increase in the local field factor at these energies.[25]

The absorbance changes of Fig. 2 are accompanied by extensive fluorescence changes for QD_{610} and QD_{546} (Insets Fig. 3). This type of quenching is reminiscent of what occurs with non-binding nitroxides such as TEMPO, with a characteristic upward curvature that can be fitted to a Perrin Model (based on the concept of the sphere of action) which in a simplistic representation assumes that only immobile quenchers with a certain radius are effective.[26] This model predicts that quenching should follow eqn (1), rather than the conventional Stern–Volmer equation.

$$\frac{I_0}{I} = \frac{\Phi_0}{\Phi} = e^{\alpha[\text{Quencher}]} \qquad (1)$$

where I_0 and I are the observable emission intensities. Thus, the exponential fitting for the ratio between areas in the absence or the presence of **1** gives α = 32.4 M^{-1} for QD_{610} and α = 103 M^{-1} for QD_{546}.

It is well known that QD quenching efficiency is size-dependent, being stronger for smaller QD.[27] Therefore, lower concentrations of **1** are needed to achieve the fluorescence quenching for QD_{546} than for QD_{610}. As expected, α is much bigger (103 M^{-1}) in this case due to the smaller size of QD_{546}.

Time resolved fluorescence studies suggest that there is a mixture of static and dynamic quenching, as illustrated in Fig. 4 where the decay traces show both a decrease of the initial maximum intensity (static) and a shortening of the lifetime (dynamic). It is common for the fluorescence decay of QD to show complex behavior and our system is no exception. We show the kinetic time profiles obtained for QD_{610} (Fig. 4A) and QD_{546} (Fig. 4B) in the absence and presence of different amounts of **1**. At higher concentrations the signal is much weaker and the analysis less reproducible.

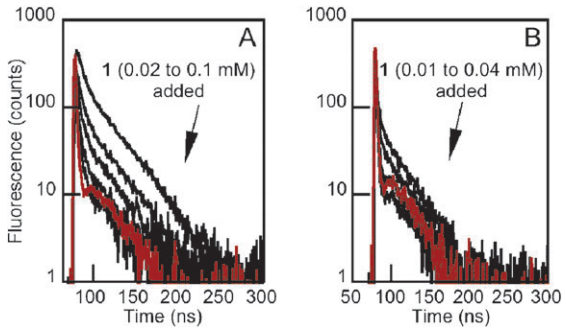

Fig. 4 (A) Kinetic time profiles of QD_{610} (0.5 μM) in toluene with different amounts of **1** (0.02 to 0.1 mM). (B) Kinetic time profiles of QD_{546} (0.5 μM) in toluene with different amounts of **1** (0.01 to 0.04 mM). Red traces are IRF.

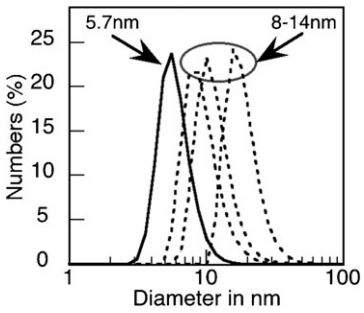

Fig. 5 Dynamic light scattering of QD_{610} (0.5 μM) in three independent measurements (dash lines) and QD_{610} to 0.3 mM of **1** (solid line).

Exponential distribution analysis (ESM) shows that the behavior is largely trimodal and this can be approximated with a triexponential function, from which average lifetimes can be calculated (Fig. S4).

A Stern–Volmer plot based on lifetimes (Fig. 3) showed a linear dependence of τ_0/τ ratio with concentration, while Φ_0/Φ has a marked positive curvature; this behaviour has been attributed to a model of quenching by a sphere of action.[28] This model interprets non-linear quenching as a mixture of dynamic and static quenching, with the latter reflecting near-contact at the time of excitation, and tends to dominate at high quencher concentrations, as it does in this case. From this plots the Stern–Volmer constants were deduced giving a $K_{SV} = 4 \times 10^4\ M^{-1}$ and $K_{SV} = 1 \times 10^4\ M^{-1}$ for QD_{610} and QD_{546}, respectively. Taking into account the fluorescence average lifetimes for QD_{610} and QD_{546} (11.9 ns and 2.3 ns respectively) the values of bimolecular quenching constants are *ca.* $\sim 10^{12}\ M^{-1}\ s^{-1}$; which, even allowing for the large dimensions of QD is significantly faster than diffusion controlled kinetics. This analysis suggests that it has to be a non-random distribution of diazonium salts in the ground state. Therefore, the diazonium salt could be in the proximity of the QD surface (whether on the actual surface or in the TOPO layer), thus altering the QD environmental charge distribution, in agreement with the absorption changes.

QD_{610} nanoparticles have a diameter of 5.2 nm (as indicated by Evident), although dynamic light scattering (DLS) gives dimensions closer to 8–14 nm of the QD emission with the instrument laser (633 nm), a rather common problem with strongly fluorescent nanomaterials. Addition of 0.3 mM **1** caused extensive fluorescence quenching, thus overcoming the problem and enabling the determination of a hydrodynamic diameter of 5.7 nm consistent with known dimensions (Fig. 5). This useful tool could be used to determinate the sizes of fluorescent particles using DLS techniques.

We asked ourselves about the possible mechanism for quenching and suspected that given the redox properties of both QD and diazonium salt, electron transfer would likely be involved;[29] that is, excited QD could transfer an electron from their conduction band leading with similar consequences as those in Scheme 1.

Such a process would involve a sacrificial role for the diazonium salt, since the only opportunity for reversal would involve the short lived diazenyl radical ($ArN_2^{\bullet}$). However, once N_2 has been eliminated there is no opportunity for reversal and the tolyl radical could bind to a Zn site right on the surface.[29] Indeed, as illustrated below, our results show that the quenching can be completely reversed upon continuous illumination of the "quenched" QD with either UVA (centered at 350 nm) or visible light (Fig. S5) after 2 h (Fig. S6). The fluorescence recovery is a first order kinetic process either under nitrogen ($k = 0.034 \pm 0.001\ min^{-1}$ or air $k = 0.020 \pm 0.001\ min^{-1}$).

A second addition of fresh diazonium salt leads to quenching, but the level of quenching is roughly one half of that achieved with fresh QD. Fig. 6 illustrates these changes for QD_{610} whereas QD_{546} are shown in Fig. S7. When these QD are irradiated, 100% fluorescence recovery is again achieved, while a third addition of **1** results in no further quenching. Examination of Fig. 6 leads to several important conclusions. First, the diazonium salt must modify the QD surface following fluorescence recovery, since otherwise a second addition of quenching would lead to similar quenching as the initial addition; clearly this is not the case, and the particles have "memory" of past quenching-recovering processes. Second, the fact that 0.02 mM concentrations of **1** are sufficient to completely prevent quenching when the third addition of **1** is made suggest that 0.04 mM of **1** (in two additions) is sufficient to completely protect all quenchable sites on the QD surface. Recovery of the emission and modification of the QD surface as in Fig. 6 leads to a minor (3 nm) blue shift in the fluorescence spectrum of QD_{610}, but suggests a minor decrease in particle size or reorganization of the surface. In any event this effect is very minor.

We note that the fact that fluorescence recovery occurs both with UV and visible light confirms that the process is initiated by QD excitation and not direct diazonium salt photolysis, since the diazonium salt is transparent in the visible region. If the fluorescence reversal is carried out in presence of a DC magnetic field the recovery is faster, which supports a radical mediated process (see Fig. S8).

A detailed ^{1}H-NMR study together with the spectroscopic results shows that prior to irradiation, there are different signals in the aromatic region that can be attributed to different environments for **1** after adsorption (see Fig. 7b). However, upon illumination all the aromatic signals collapsed to one that could be easily assigned to single *para* aromatic system (Fig. 7c). We had hoped that the aryl group would

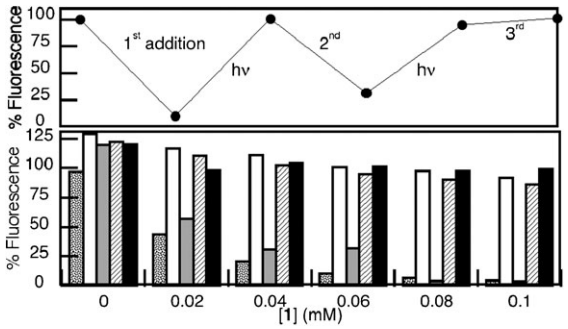

Fig. 6 Bottom: Evolution of QD_{610} (0.5 μM) fluorescence in toluene with different concentrations of **1** after the first addition ■, first irradiation □, second addition ■, second irradiation ■ and third addition ■. Top: detail for QD_{610} with 0.06 mM of **1**; the horizontal axis corresponds to subsequent stages of the experiment. Irradiations correspond to 2h of UVA exposure.

remain bound to the surface. However, ^{1}H-NMR, ^{19}F-NMR and ^{11}B-NMR results were consistent with the presence of *p*-difluoroboranetoluene **2** in the reaction mixture (see Fig. 1). Aryl-Zn in presence of Lewis acids, such as BF_3, have been reported to produce **2**.[30,31] Our results indicate that as soon as the aryl group is bound to the QD surface, it leads to **2**, which could possible form a complex with the S present in the QD shell (Scheme 2).

In fact, **2** can be easily removed from the media if the QD are precipitated with methanol due to the higher affinity of boron for oxygen than for sulfur. A possible explanation for the QD protection against subsequent quenching would involve surface modification due to the F group attached to the zinc atoms.

On the other hand, the treatment of QD_{610} with **1** (additions and subsequent irradiations) changes the response against

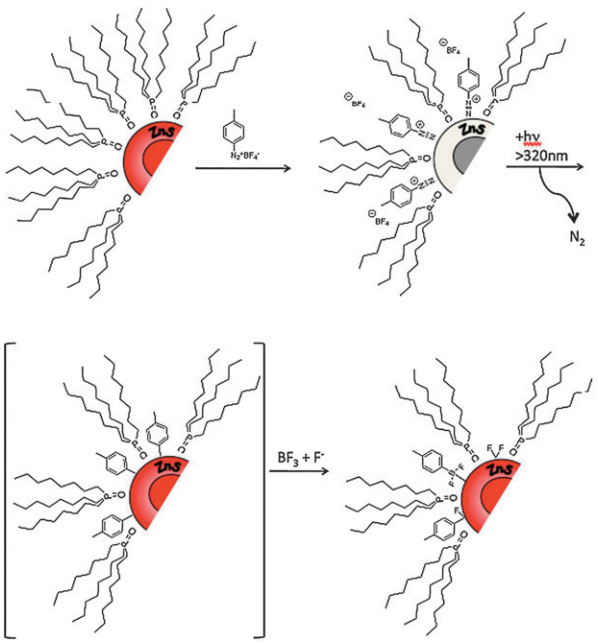

Scheme 2 Proposed mechanism for the interaction between QD_{610} and **1**.

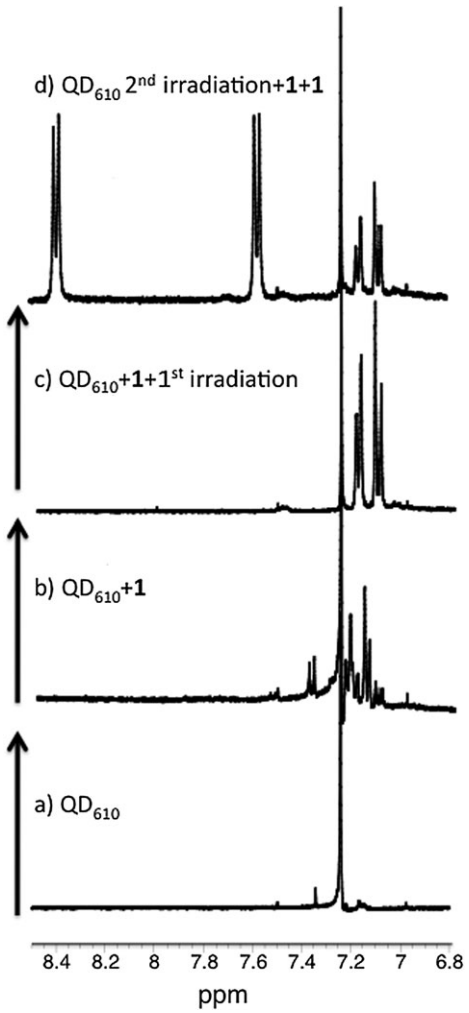

Fig. 7 ^{1}H-NMR spectral evolution in the aromatic region (8.5–6.8 ppm) for (a) QD_{610}, (b) QD_{610} with 0.1 mM of **1**, (c) QD_{610} with 0.1 mM of **1** after irradiation and (d) QD_{610} after second addition of 0.1 mM of **1**, second irradiation and then addition of 0.2 mM of **1**.

other quenchers such as 4-amino TEMPO (**4aT**).[27] Quenching of TOPO-capped core shell QD by **4aT** has a characteristic bimodal behaviour. The first type of quenching, at low quencher concentrations, is due to a presence of vacancies in the ZnS shell and, at high concentrations is characteristic of the exchange of TOPO. Fig. 8 shows the comparative Stern–Volmer plot for the quenching of QD with and without treatment with **1** by **4aT**. Our result cleary shows a change in both types of quenching, which also argues for surface modification.

While illustrated with core–shell QD, a similar quenching behavior is also observed in the case of core-only CdSe, QD_{558} (synthesized by Peng's method).[32] In this case much lower concentrations of **1** are required, as already observed in other quenching studies for core-only particles (see Fig. S9–S10). That is, the shell offers considerable protection toward quenching by molecules in solution. However, the quenching reversal does not take place in this case due to the unstability of core CdSe QD upon irradiation.[33]

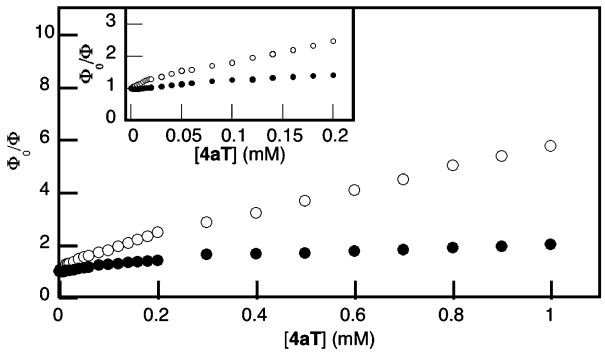

Fig. 8 Stern–Volmer plot of a QD_{610} solution (0.5 μM) in toluene with (●) and without (○) treatment with **1**. Inset: expansion of Stern–Volmer plot at low **1** concentrations.

Conclusion

Overall our results lead us to conclude that diazonium salt provides an easy route for the modification and protection against quenching for core–shell CdSe/ZnS QD. However, this method does not lead to aromatic surface modification under our conditions. Beyond this conclusion, we have learned that diazonium salt treatment offers a simple experimental "trick" to facilitate DLS measurements where under normal conditions these measurements are sometimes prevented by fluorescence interference. Further, diazonium quenching occurs by a combination of static and dynamic processes that can be fitted with a Perrin model in a similar manner as non-binding nitroxides. Upon photoexcitation an electron transfer proccess from the QD to the diazonium salt leads to the generation of aryl-Zn species which in the presence of BF_3 gives rise to *p*-difluoroboranetoluene. Once all the quencheable sites on the QD surface have been used, diazonium salt cannot quench the QD anymore and this new protected surface has attenuated reactivity towards other quenchers, such as **4-aT**.

We thank the Natural Sciences and Engineering Research Council of Canada, the Spanish Ministry of Science and Innovation, FECYT, CFI and the Government of Ontario for support. We also thank Dr Natalia Pacioni for her helpful comments.

Notes and references

1 A. P. Alivisatos, *Science*, 1996, **271**, 933–937.
2 C. Burda, X. B. Chen, R. Narayanan and M. A. El-Sayed, *Chem. Rev*., 2005, **105**, 1025.
3 H. J. Eisler, V. C. Sundar, M. G. Bawendi, M. Walsh, H. I. Smith and V. I. Klimov, *Appl. Phys. Lett*., 2002, **80**, 4614–4616.
4 Y. Xing, Q. Chaudry, C. Shen, K. Y. Kong, H. E. Zhau, L. W. Chung, J. A. Petros, R. M. O'Regan, M. V. Yezhelyev, J. W. Simons, M. D. Wang and S. Nie, *Nat. Protoc*., 2007, **2**, 1152–1165.
5 M. A. Schreuder, K. Xiao, I. N. Ivanov, W. S. M. and S. J. Rosenthal, *Nano Lett*., 2010, 573–576.
6 P. O. Anikeeva, J. E. Halpert, B. M. G. and V. Bulovic, *Nano Lett*., 2009, **9**, 2532–2536.
7 M. Derfus, W. C. W. Chan and S. N. Bhatia, *Nano Lett*., 2004, **4**, 1–18.
8 B. O. Dabboussi, J. Rodriguez-Viejo, F. W. Mikulec, J. R. Heine, H. Mattoussi, R. Ober, K. F. Jensen and M. G. Bawendi, *J. Phys. Chem. B*, 1997, **101**, 9463–9475.
9 X. Michalet, F. F. Pinaud, L. A. Bentolila, J. M. Tsay, S. Doose, J. J. Li, G. Sundaresan, A. M. Wu, S. S. Gambhir and W. S., *Science*, 2005, **307**, 538–544.
10 C. Querner, P. Reiss, J. Bleuse and P. A., *J. Am. Chem. Soc*., 2004, **126**, 11574.
11 F. Pinaud, D. King, H. P. Moore and W. S., *J. Am. Chem. Soc*., 2004, **126**, 6115–6123.
12 S. Kim and M. G. Bawendi, *J. Am. Chem. Soc*., 2003, **125**, 14652–14653.
13 J. C. Scaiano and N. Kim-Thuan, *Can. J. Chem*., 1982, **60**, 2286–2291.
14 J. Pinson and F. Podvorica, *Chem. Soc. Rev*., 2005, **34**, 429–439.
15 M. S. Strano, C. A. Dyke, M. L. Usrey, P. W. Barone, M. J. Allen, H. Shan, C. Kittrell, R. H. Hauge, J. M. Tour and R. E. Smalley, *J. Am. Chem. Soc*., 2003, **131**, 1519–1522.
16 C. A. Dyke and J. M. Tour, *Nano Lett*., 2003, **3**, 1215–1218.
17 B. K. Price, J. L. Hudson and J. M. Tour, *J. Am. Chem. Soc*., 2005, **127**, 14867–14870.
18 D. Ghosh and S. Chen, *J. Mater. Chem*., 2008, **18**, 755–762.
19 M. P. Stewart, F. Maya, D. V. Kosynkin, S. M. Dirk, J. J. Stapleton, C. L. McGuiness, D. L. Allara and J. M. Tour, *J. Am. Chem. Soc*., 2004, **126**, 370–378.
20 W. W. Yu, L. Qu, Q. Guo and X. Peng, *Chem. Mater*., 2003, **15**, 2854.
21 M. González-Béjar, M. Frenette, L. Jorge and J. C. Scaiano, *Chem. Commun*., 2009, 3202–3204.
22 M.P. Doylez and W. J. Bryker, *J. Org. Chem*., 1979, **44**, 1572–1574.
23 T. Blaudeck, E. I. Zenkevich, F. Cichos and C. v. Borczyskowski, *J. Phys. Chem. C*, 2008, **112**, 20251–20257.
24 B. J. Walker, G. P. Nair, L. F. Marshall, V. Bulovic and M. G. Bawendi, *J. Am. Chem. Soc*., 2009, **131**, 9624–9625.
25 I. Moreels and Z. Hens, *Small*, 2008, **4**, 1866–1868.
26 M. Laferriére, R. E. Galian, V. Maurel and J. C. Scaiano, *Chem. Commun*., 2006, 257–259.
27 J. C. Scaiano, M. Laferrière, R. E. Galian, V. Maurel and P. Billone, *Phys. Status Solidi A*, 2006, **203**, 1337–1343.
28 J. R. Lakowicz, *Principles of Fluorescence Spectroscopy*, Springer Science + Business Media, LLC, 2006.
29 M.-C. Bernard, A. Chauss, E. Cabet-Deliry, M. M. Chehimi, J. Pinson, F. Podvorica and C. Vautrin-Ul, *Chem. Mater*., 2003, **15**, 3450–3462.
30 K. Torssell, *Acta Chem. Scand*., 1954, **8**, 1779–1786.
31 P. A. McCusker and H. S. Makowski, *J. Am. Chem. Soc*., 1957, **79**, 5185–5188.
32 Z. A. Peng and X. Peng, *J. Am. Chem. Soc*., 2002, **124**, 3343.
33 L. Rene-Boisneuf and J. C. Scaiano, *Chem. Mater*., 2008, **20**, 6638–6642.

